CAVITATION EROSION PREDICTION ON FRANCIS TURBINES-PART 3 METHODOLOGIES OF PREDICTION

J.M. DOREY, E. LAPERROUSAZ
Electricité de France
6, Quai Watier, 78401 CHATOU Cedex, France
F. AVELLAN, P. DUPONT
IMHEF/ EPFL
33 Avenue de Cour, CH 1007 Lausanne, Switzerland
R. SIMONEAU, P. BOURDON
Hydro-Québec
1800 boul. Lionel Boulet, Varennes, Québec, Canada J3X 1S1

Summary: In the frame of a joint research programme between EDF, Hydro-Québec and IMHEF, different methods are investigated to predict cavitation erosion on Francis turbines from model. They are based on measurement of pitting, pressure fluctuations and acceleration. The measurement techniques have been detailed in Part 1 and Part 2. The present article describes essentially the theoretical and practical aspects of the methods and discusses the results obtained until now from the model and prototype tests. The first analysis shows that the methods proposed are suitable to measure cavitation aggressiveness on model and on prototype, and that the level on the model is several orders of magnitude smaller than on the prototype. To adjust transposition laws, a more complete set of data is needed.

1. Introduction

Despite many efforts in the past, cavitation erosion still remains an unsolved problem regarding the acceptance tests on model for hydraulic turbines including Francis turbines. The different methods used today to fix acceptable tailwater level from cavitation model tests (to add a " safety margin" to the efficiency drop tailwater level, to fix a certain acceptable cavity length, to use paint erosion tests or so)do not give full satisfaction since they involve empirical experience and subjective considerations.

As this problem remains essential for sizing and design of hydraulic turbines, EDF, HydroQuébec and EPFL have conducted an important research programme on this subject, including tests on a 260 MWe Francis Turbine and its model. The programme has been previously presented [1]. The measurements of cavitation intensity on the prototype and on the model are described in Part 1 and Part 2.

E. Cabrera et al. (eds.), Hydraulic Machinery and Cavitation, 564–573.

2. Cavitation aggressiveness and model-to-prototype similitude

2.1. CAVITATION AGGRESSIVENESS

It must be reminded that cavitation erosion is the result of accumulation of impacts due to the collapse of vapour "structures" near the wall. So cavitation erosion can be split in two different mechanisms :

- first, the hydraulic mechanism: local depression in the flow generates vapour structures, growing and then collapsing, leading to minute impacts on the wall;
- second, the damage mechanism: under cavitation impacts the wall material is damaged, ending with mass removal.

The interface between these two distinct phenomena is called the "cavitation aggressiveness", which is the impact loading applied on the wall by successive collapses. In a first approach, it can be set that cavitation aggressiveness is the pure consequence of the first mechanism and the input of the second.

So the cavitation aggressiveness can be defined as a set of impacts striking the wall, each impact being characterized by its pressure P_i, its duration t_i, and the characteristic size L_i of the surface stroked. Although the mechanisms of collapse are not yet fully elucidated, it is admitted now that these parameters are in the range of gigaPascal for P_i, microsecond for t_i, and 0.1-1 mm for L_i. Up to now, no on-line instrumentation is able to measure cavitation aggressiveness, and the methods proposed hereafter are based on indirect measurements.

2.2. MODEL TO PROTOTYPE SIMILITUDE

Here we remind only the main features of the reasoning leading to scaling laws. More argued statements of these laws can be found in [2]. Between a prototype (reference size: L_{proto} , speed : N_{proto}) and its model (reference size: L_{model} , speed : N_{model}), the hydraulic mechanism can be theoretically ruled by scaling relationships:

- The extend of cavitation area: the well known Sigma similitude between model and prototype theoretically ensures that similar areas are under vapour pressure;
- The size of vapour transient cavities: since cavitation extent is similar, the size of cavities is also similar, i.e. proportional to the scale;
- The rate of production of vapour cavities: if they are produced by a pocket attached on the wall, or by a vortex shedding, their rate of production follows a constant Strouhal number. If the vapour structures are generated by nuclei, this rate will be proportional to the number of nuclei per volume unit;
- The potential power of vapour structures: it is the product of their potential energy (i.e. the volume multiplied by the pressure that forces the collapse minus vapour pressure) by their rate of production. Since size, pressure and rate can be scaled, this also can be scaled.
- The cavitation impacts on the wall: the impact being considered as a shock, the impact pressure P_i due to the collapse of a vapour cavity can be scaled by $\rho c V$

(ρ = water density, **c** = sound velocity in water, **V** = reference flow velocity), while the impact size L_i and the time t_i can be scaled by the size of the vapour cavity i.e. by the homology factor.

With these considerations in mind, aggressiveness can be transposed from model to prototype.

On the contrary, the loss of mass under cavitation aggressiveness cannot be ruled by similitude laws. Up to now, too little is known on the processes involved in material damage to lay down a simple modelisation.Experimental data are still needed. These may be provided by devices such as water jet [4] or vortex generator [8], or others.

3. Prediction methods and results

3.1. PREDICTION USING PITTING MEASUREMENTS

3.1.1 *Requirements for pitting tests*

This method is based on the analysis of cavitation pitting obtained after a short duration test (less than an hour) on polished samples made of soft metal (pureCu, pure Al, Ag or so) mounted on the model. The test is run in hydraulic similitude with investigated prototype operating conditions, including cavitation similitude.

To get the highest cavitation aggressiveness, it is important to reach the highest head possible on the model platform. This will be favourable for transposition, to get a sufficient pitting, and to diminish extraneous effects such as damping due to air content, and viscous effects. It is often impossible to reach the same head on the model as on the prototype, but a head of about one half to one quarter the prototype one seems to be a good range. Air content in the water of the loop has to be reduced as low as possible to avoid any damping effects on the collapse.

Preliminary tests are required to fix test duration that must be long enough to get a representative pitting , but not too long to avoid excessive overlapping of pits.

3.1.2. *Techniques and apparatus*

The easiest way to put soft polished metal in the erosion area is to use samples mounted in the blades. If this technique has been successful on the prototype, unfortunately, on the model, preliminary tests with pure aluminium samples shows undesirable cavitation pitting behind small discontinuities (less than 0.2 mm height) between sample and blade. Electrolytic deposition of metal directly on the blades is found safer but it rules out the use of Al (poor quality of deposits) and Cu (variable hardness of deposits). In this case, silver has been found to be suitable.

As for pitting measurement, we used a UBM laser profilometer that provides a mapping of the surface. After levelling, pitting can be extracted by a software named "Adresse" that determines the values of pit depth h_i, pit radius R_i, and pit volume V_i for each pit. This process is detailed in [3]. This software calculates also

the pressures and sizes, and perfoms the transposition from model to prototypeaccording to the laws set out hereafter.

3.1.3. *Transposition procedure*

After a test duration T, pitting obtained is measured on a surface $S_{a\,mod}$ and provides a set of pits $(h_i, R_i)_{mod}$, each one being characterized by its depth h_i and radius R_i. From the pits geometry and the material properties (simple shear stress S_0, elastic Young modulus **E**, Poisson modulus ν, sound velocity C_s), pressure P*i* and size L*i* of the corresponding impact can be deduced using the following relationship obtained by analysis of elastoplastic deformation [5] [6]:

$$\frac{R_i}{L_i} = f_1\left(\frac{C_l}{L_i}\cdot dt\right) \qquad \text{and} \qquad \frac{h_i}{L_i} = \frac{S_0}{E}\cdot\left(\frac{P_i}{S_0}\right)^m \cdot A^{1-m}$$

where $A = f_2\left(\frac{C_l}{L_i}\cdot dt, \nu\right)$, $m = f_3\left(\frac{C_s}{L_i}\cdot dt, \frac{C_l}{L_i}\cdot dt\right)$, C_l is the sound velocity in the water and **dt** is the time duration of the impact. f_1 , f_2 and f_3 are determined by numerical simulation of plastic deformation, $C_s dt / L_i$ and $C_l dt / L_i$ can be assumed to be constant [7]. So the relationship can be written in the following form :

$$(P_i, L_i) = f_{mat}(h_i, R_i)$$

where f_{mat} depends only of the material.

This provides the set of impacts $(P_i, L_i)_{mod}$ obtained on the model.

Given : - the scale ratio $\lambda = L_{proto} / L_{mod}$, and
- the speed ratio $n = N_{proto} / N_{mod}$

of the model, this set $(P_i, L_i)_{mod}$ is then transposed to prototype $(P_i, L_i)_{proto}$ by means of the following scaling laws:

$$P_{i\,proto} = P_{i\,mod} \cdot \lambda \cdot n \quad \text{and} \quad L_{i\,proto} = L_{i\,mod} \cdot \lambda$$

This deduced aggressiveness $(P_i, L_i)_{proto}$ is supposed to be applied on a surface:

$$S_{a\,proto} = S_{a\,mod} \cdot \lambda^2 \quad \text{during a time } T_{proto} = T_{mod} / n$$

These relations are deduced from the similitude considerations mentionned above, with the hypothesis of constant Strouhal number for production of cavities.

With the inverse relationship f_{mat}^{-1} between pressure pulse and pit, one can calculate pitting $(h_i, R_i)_{proto}$ that would be produced by this aggressiveness $(P_i, L_i)_{proto}$ on the prototype, on the prototype material. A volume pitting rate can be inferred:

$$V_d = \Sigma V_i / (S_{a\,proto} \cdot T_{proto})$$

where V_i is the volume of pit *i* ($V_i = f(h_i, R_i)$).

Finally, erosion on the prototype is deduced using correlations between pitting and mass loss obtained in laboratory (high pressure cavitating jet or venturi) for a range of impulse pressures and materials:

$$Er = f(V_d, \text{material})$$

3.1.4. *Pitting Results*

The pitting obtained on the prototype is described in Part I and in a previous paper[4]. What must be noticed here is the very large size of the larger pits: up to 2 mm diameter despite the hardness of the material (316L stainless steel). This confirms the assumption on scale of pits proportional to the size of the machine.

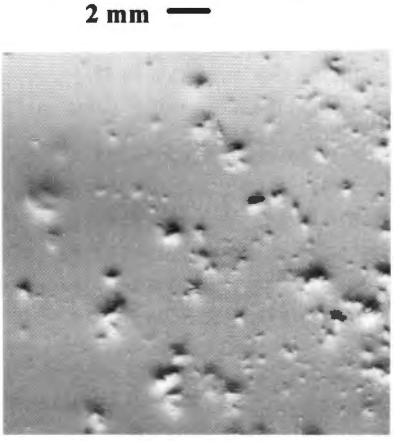

Figure1: typical pitting on the prototype on 316L SS (130 HB)

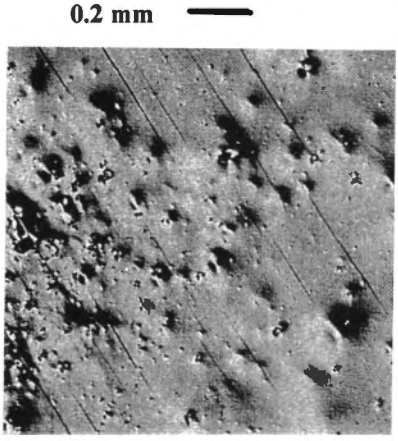

Figure 2 : pitting obtained on the model on pure aluminium (16 HB)

On the model, preliminary tests have been carried out with aluminium samples flush mounted on two blades. After a short duration, a good pitting was obtain, even if on some samples parasite cavitation was observed. This can be seen in figure 2.

Nevertheless, these preliminary tests are not strictly comparable to the prototype tests since, as explained in Part 2, the model is not exactly representative and the cavitation behaviour is different from the prototype, what forbid direct comparison.

3.1.5. *Tentative transposition*

Despite this fact, an interesting exercise can be carried out using the prototype results : from measurements on stainless steel on sample 2 (one of the more severely damaged, $\sigma = 0.120$, $\phi = 0.27$, vane opening 78%) one can use the inverse procedure to predict what is expected on the model. The test lasted $T_{proto} = 30$ mn. The sample 2 was analysed on $S_{proto} = 100\ mm^2$ and gives the following results:

- number of pits : 193
- total volume of pits: $V_{tot} = \Sigma V_i = 4.35\ 10^8\ \mu m^3$

From the pits set (h_i, R_i, V_i) the following values are calculated:

- mean weighted depth: $h_v = \Sigma(h_i.V_i)/\Sigma V_i$
- mean weighted radius: $R_v = \Sigma(R_i.V_i)/\Sigma V_i$
- volume pitting rate: $V_d = V_{tot}/(S_{proto}.T_{proto})$

These values are listed in table 1, as for the successive steps of the transposition.

Then, the mechanical characteristics of 316 L stainless steel beeing $S_0 = 400$ MPa, $E = 200$ GPa, $C_s = 5800$ m/s, the inferred pressures P_i and size L_i of impacts are calculated. They range from 1.9 to 4.5 Gpa on the prototype. Transposition is then applied. Since the model scale is $\lambda = 14.66$ and $n = 0.1125$, pressures are divided by 1.65, while sizes are divided by 14.66. The corresponding surface and duration are:

$$S_{mod} = S_{proto} / \lambda^2 = 0.465 \text{ mm}^2 \quad \text{and} \quad T_{mod} = T_{proto} \cdot n = 3.36 \text{ mn}.$$

Once aggressiveness is transposed, one can calculate the pitting on the model, for a given material with the software "Adresse". On the same material (316L SS), the pitting obtained is described in column 2 of Table 1. What is significant is that, while the radius R_v decreases almost proportionally to the scale, the depth is divided by more than four time the scale. Most of such pits would be hard to measure. The weakness of the aggressiveness on the model justifies the use of a softer material.

The same aggressiveness (set (P_i, L_i)) applied on pure Al ($S_0 = 100$ MPa, $E = 50$ GPa, $C_s = 5000$ m/s) leads to the pitting described in column 3 of Table 1. Here, the pitting is very important since many pits are deeper than large. This seems to be unrealistic. It can be compared with the pitting obtained during one of the preliminary tests on the model ($\sigma = 0.07$, $\phi = 0.27$, vane opening 78%)). After a test duration of 15 mn, a 9 mm^2 surface of one of the most eroded samples has been analysed and the results are given in column 4 of Table 1. The pitting is much lower, pits are less deep and larger than expected but the similitude conditions are not respected (specially σ similitude), so that no conclusion can be drawn up to now. More experimentation is currently carried out, using silver coating of the blades. At the present time, the results show clearly that pitting measurements on model can be obtained, and that transposition has to be adjusted.

Table 1 : Results of transposition from prototype pitting tests

	Prototype tests on 316L SS	Transposed to the model on 316L SS	Transposed to the model on Al 59	Model test on Al 59
Duration (mn)	30	3.36	3.36	15
Surface (mm^2)	100	0.465	0.465	9
hv (μm)	22.2	0.207	36	1.9
Rv (mm)	0.66	0.045	0.045	0.17
V_d (μm/s)	$1.29\ 10^{-3}$	$1.07\ 10^{-4}$	$2.05\ 10^{-2}$	$6.2\ 10^{-4}$
(mm/hour)	$4.66\ 10^{-3}$	3.8710^{-4}	0.074	$0.223\ 10^{-2}$

3.2. PREDICTION USING VIBRATION ANALYSIS

This method aims to measure the amplitude of shock forces applied on the blades by cavitation. Since direct measurement is not possible, a method is proposed to infer these forces from the signal of an accelerometer mounted outside the machine. To avoid extraneous noises from mechanical phenomena or flow, forces are calculated

in a high frequency range. The transfer function from the blades where cavitation occurs to the measurement spot can be determined by two different means : spark generator and instrumented impact hammer. From energy considerations, it can be said that inferred forces F_{mod} obtained on the model can then be transposed to the prototype using the following formula:

$$F_{proto} = f(\lambda,n) \cdot F_{mod}$$

where λ is the scale ratio between prototype and model, and **n** is the speed ratio.

That such a relation or another may exist rests on the following considerations. Developed forces for similar flows on model and prototype should scale with the energy of cavities, i.e. their volume. The rate of collapse of these cavities on the runner must also be considered as this parameter may vary between model and prototype and influences the inferred forces values.

With the results of both campaigns in hand, we identify scaling law on the basis of the calibrated values of the mean square inferred high frequency forces. From the knowledge of the damaged areas on the prototype, the inferred forces values can be converted to erosion rates using erosion data obtained on a laboratory jet.

Transmissibility functions (ratio of response acceleration power spectrum to input force spectrum) were measured between the lower guide bearing and the eroded a reason the blades by a reciprocity instrumented hammer impact method. An average response was established by measuring the response of 5 blades on the prototype and 4 on the model with the runner under water in both cases. The 0-25 and 0 -100 kHz frequency ranges were utilized respectively on the prototype and on the model. The useable frequency ranges where adequate coherence (>.8) between the response and the excitation were realized were 0-16kHz on the prototype and 0-80kHz on the model. The need to measure the transmissibility function with the runners in water was confirmed by the significant differences between values measured with the runners in air or in water. On the prototype, smaller values were seen with the runner in water, as anticipated, due to the coupling of vibration energy from the runner blades to the water while the opposite was true on the model where increased coupling from the lower guide bearing to the runner is achieved with the presence of water in the runner crown to bearing gap.

Forces were inferred on the prototype in the .8 to 11.296 kHz as had been done but this time with the transmissibility function measured with the runner underwater. This produces substantially higher force levels than estimated in the previous measurement campaign. On the model, the 20 to 35 kHz range was utilized because of interfering high frequency vibration at the lower guide bearing generated by a 90° 1 to 1 gearbox linking the model shaft to the generator. This underestimates the real force values by a factor of at least 2 or 4. The presence of these undesirable vibrations is inconsistent with reciprocity measurement approach and will be eliminated in the future tests. The results of the prototype inferred force calculations are summarized in figure 3 with maximum values observed on the prototype at 90% guide vane opening with high downstream levels. Figure 4 shows the correlation with volume pitting rate. The highest level on the model is also obtained at 90%

guide vane opening but the inferred forces per unit area on the model are four to five times much weaker than on the prototype.

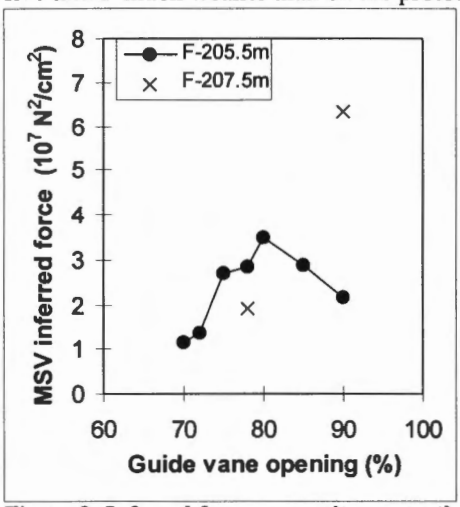

Figure 3: Inferred forces per unit area on the proto (lower guide bearing acceleration)

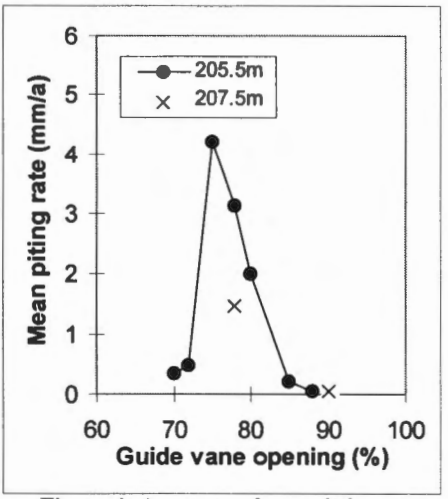

Figure 4: Average volume pitting rate on 4 disks for same tests on the proto.

Cavitation characteristics on the model however appear to differ slightly from those observed on the prototype. The high frequency acceleration amplitude modulation spectra at the lower guide bearing and in the crown of the runner show that impacts occur at the guide vane passing frequency as on the prototype but modulation components of similar amplitude are also present at the blade passing frequency. This confirms that flow conditions are not fully homologous to those of the prototype as discussed in Part 2.

3.3. PREDICTION USING ELECTROCHEMICAL PROBE DECER

This method based on electrochemical effects during cavitation erosion can give a good representation of cavitation aggressiveness through the activation current delivered by the titanium electrochemical probe which is directly proportional to the actual erosion rate [8]. This localized on-line measurement on both prototype and model is a complement to pitting results to provide the influence of operating parameters on cavitation aggressiveness. On the prototype, this method gives similar results than the others methods, with maximum erosion near optimum opening The maximum current measured is in the range of 3 μA for a 7.5cm^2 of a grade 2 Titanium. (This corresponds to 20 mm/year erosion on Ti grade 2 according to laboratory jet tests [8]). On the model, the maximum current level detected on Ti49 is 0.05μA on a surface of 0.32 cm^2. This is very low and correspond to 0.16 mm/year of Titanium erosion (according to laboratory jet tests [8]). Since the

resistance of Ti 49 is ten times lower than Ti grade 2, it means that cavitation erosion found on the model seems to be about 1000 less than on the prototype.

3.4. PREDICTION USING CAVITATION EROSIVE POWER

It has been set previously (Avellan *et al*) that the cavitation erosive power could be evaluated from energy dissipated by collapses of transient cavities and their production rate. This power can be expressed as :

$$P_{er} = \frac{1}{2} K \cdot \rho \cdot \left(c_{p\,max} + \sigma\right) \cdot C_{ref}^3 \cdot St \cdot \frac{V_c}{L_c}$$

where $\mathbf{c_{p\ max}}$ is the maximum pressure coefficient in the recovering pressure region downstream the main cavity, σ the cavitation coefficient, $\mathbf{C_{ref}}$ a velocity reference, **St** the Strouhal number corresponding to the production rate of the transient cavities, $\mathbf{L_c}$ the main cavity length, $\mathbf{V_c}$ the transient cavities volume and **K** a scaling constant. This parameter can be calculated on the model using visualisation to determine $\mathbf{V_c}$, $\mathbf{L_c}$ and **St**, and transposed from the model to the prototype.
Hydraulic similitude and sigma similitude will ensure that $\mathbf{c_{p\ max}}$, σ and **St** are the same on the model and on the prototype. Then it can be assumed that $\mathbf{L_c}$ is proportional to the reference length **L**, and that $\mathbf{C_{ref}} \propto N \cdot L$ (**N** : rotational speed)
As for $\mathbf{V_c}$, two hypothesis can be proposed:

- if it is assumed that $\mathbf{V_c}$ is proportional to $\mathbf{L^3}$, then the ratio between erosive power between model and prototype can be written:

$$\frac{P_{proto}}{P_{model}} = \left(\frac{C_{ref\ proto}}{C_{ref\ model}}\right)^3 \cdot \frac{V_{c\ proto}}{V_{c\ model}} \cdot \frac{L_{c\ mode}}{L_{c\ protol}} = \left(\frac{N_{proto}}{N_{model}} \cdot \frac{L_{proto}}{L_{model}}\right)^3 \cdot \left(\frac{L_{proto}}{L_{model}}\right)^3 \cdot \left(\frac{L_{proto}}{L_{model}}\right)^{-1}$$

$$r = \frac{P_{proto}}{P_{model}} = \left(\frac{N_{proto}}{N_{model}}\right)^3 \cdot \left(\frac{L_{proto}}{L_{model}}\right)^5 = n^3 \cdot \lambda^5$$

(notice: this is equal to the classical ratio on machine powers)
Since $\mathbf{n} = 0.1125$ and $\lambda = 14.66$ then in this case: $\mathbf{r} = 964$

- if the following law, established in a previous statistical study [10] is applied:

$$V_{cr} = k \cdot L_c^{2.6} \cdot C_{ref}^{-0.4}$$

then the ratio becomes:

$$r = \frac{P_{proto}}{P_{model}} = \left(\frac{N_{proto}}{N_{model}}\right)^{2.6} \cdot \left(\frac{L_{proto}}{L_{model}}\right)^{4.2} = n^{2.6} \cdot \lambda^{4.2}$$

then in this case: $\mathbf{r} = 269$

These two results emphasises clearly that, even if some uncertainty remains on the transposition laws, the cavitation intensity is much higher on the prototype than on the model. Then, to predict erosion on the prototype from transposed power, experimental correlations from reference data have to be used.

4. Conclusions

The proposed procedures to predict cavitation erosion from model tests take advantage from a campaign on a large Francis Turbine and its model.
Particular methods are set from each instrumentation type: pitting, vibration, electrochemical probe and erosive power. Results allow to confront them to actual data and to assess the hypothesis on transposition of cavitation aggressiveness. At the present time, since the programme is not completed, only partial conclusions can be drawn. Obviously the four methods proposed are able to quantify cavitation aggressiveness on the model. They all clearly show that cavitation aggressiveness is much smaller on the model than on the prototype, and this is due to less energetic collapses, due to the reduction of both pressures and sizes of impacts.
As for a definitive assessment of transposition and prediction processes, the completion of the programme is needed for a thorough synthesis.

References:

[1] E. Laperrousaz et al, 1994 "Prediction cavitation erosion in Francis turbines on the basis of scale model testing", *Proc. 17th IARH Symposium*, Beijing, China.
[2]Y. Lecoffre, P. Grison;, J.M. Michel , 1986 "Prevision de l'érosion de cavitation pour les turbomachines " *Proc. 14th IARH Symposium*, Montreal, Canada.
[3] J.M. Dorey, R. Simoneau ,P. Bourdon, M. Farhat, F. Avellan 1994 "Quantification of cavitation aggressiveness in three different dvices using accelerometer, DECER, and pitting measurements" , *Proc.Second International Symposium on Cavitation*, Tokyo, Japan.
[4] P. Bourdon, R. Simoneau, J.M. Dorey, 1994 "Accelerometer and pit counting detection of cavitation erosion on a laboratory jet and a large Francis tu rbine" *Proc. 17th IARH Symposium*, Beijing, China.
[5] R. Fortes-Patella, J.L. Reboud, J.M. Dorey, 1991 "Simulation of cavitation impact damageon an elastoplastic solid", *Proc. ASME Cavitation and Multiphase Flow Forum*, Portland, USA.
[6] R. Fortes-Patella ,J.L. Reboud , 1992 "Analysis of cavitation erosion by numerical investigation of solid damage" *Proc. 16th IARH Symposium* , Sao-Paulo, Brasil.
[7] R. Fortes-Patella ,J.L. Reboud, 1995 "A new approach to evaluate cavitation erosion power" *Proc. International Symposium on Cavitation*, Deauville, France.
[8] R. Simoneau ,P. Bourdon, M. Farhat, F. Avellan, J.M. Dorey, 1993 "Cavitation erosion, impact intensity and pit size distribution of jet and vortex cavitation", *Proc. ASME annual winter meeting, Bubble noise and cavitation erosion in fluid systems* , New Orleans, USA.
[9] R. Simoneau, 1995 "Cavitation pit counting and steady state erosion rate" *Proc. International Symposium on Cavitation*, Deauville, France.
[10] F. Pereira, Ph. Dupont, F. Avellan, 1995 "A statistical approach to the study of transient erosive cavities on a 2D profile" *Proc. ASME annual meeting* , South Carolina, USA.